Compton scattering studies of electron correlation effects in chromium

1989 J. Phys.: Condens. Matter 1 541

(http://iopscience.iop.org/0953-8984/1/3/005)

J. Phys.: Condens. Matter 1 (1989) 541–550. Printed in the UK

Compton scattering studies of electron correlation effects in chromium

D A Cardwell†, M J Cooper and S Wakoh‡
Department of Physics, University of Warwick, Coventry CV4 7AL, UK

Received 25 July 1988

Abstract. The [100], [110] and [111] directional Compton profiles of chromium have been measured with both 412 keV and 60 keV γ-radiation. When compared with the augmented plane-wave (APW) or linear combination of atomic orbitals band models, all three profiles show an expansion of the electron density distribution attributed to electron–electron correlation and most marked along the [111] nearest-neighbour direction. A new method of calculating anisotropic correlation effects in Compton profiles, which is based on the three-dimensional APW density of states, is reported and shown to reconcile experiment and theory.

1. Introduction

The Compton scattering technique has been applied to the study of cubic 3d metals with the objective of testing the accuracy of band-structure models of the ground-state electron momentum density $n(\boldsymbol{p})$. Projections of this distribution, given by $J(p_z)$ in equation (1), can be deduced from the spectral distribution of Compton scattering $\mathrm{d}^2\sigma/(\mathrm{d}\Omega\,\mathrm{d}\omega)$ if the interaction can be treated within an impulse approximation. Then

$$\frac{\mathrm{d}^2\sigma}{\mathrm{d}\Omega\,\mathrm{d}\omega} \propto J(p_z) = \int\int n(\boldsymbol{p})\,\mathrm{d}p_x\,\mathrm{d}p_y \tag{1}$$

where the z axis is along the x-ray scattering vector and $J(p_z)$ is known as the Compton profile. It is the sensitivity of this quantity to the behaviour of the valence electron that makes it particularly interesting [1].

In principle, $n(\boldsymbol{p})$ can be reconstructed from a number of these projections [2] but this has rarely been attempted with Compton data because of the long time involved in acquiring each profile; however, that situation is changing with the development of focusing spectrometers associated wth synchrotron or x-ray tube sources. It is usual to isolate the aspherical part of the distribution by forming directional difference profiles $\Delta J(p) = J_{hkl}(p_z) - J_{h'k'l'}(p_{z'})$ which has the practical advantage of eliminating many of the troublesome systematic errors. If reliable corrections can be made, individual profiles

† Present address: Plessey Research (Caswell) Laboratories, Caswell, Towcester, Northants, NN12 8EQ, UK.

‡ Present address: University of Library and Information Science, Tsukuba, 305 Japan.

0953-8984/89/030541 + 10 $02.50

can be compared with model predictions and this has proved to be the most effective way of highlighting the limitations of the independent particle approximation.

Iron and vanadium [3, 4], copper [5, 6] and nickel [7] have been studied in this way. In all cases, inspection of the directional difference profiles show that band theories consistently overestimate the scale of the anisotropies, independently of the degree of sophistication of the model. Ruling out the possibility of common systematic errors (for nickel the experiments were performed in two laboratories and vanadium was the object of an international project involving at least four laboratories) the most likely origin of the discrepancy is the neglect of electron–electron correlation effects in the band models (i.e. correlation effects not included in the Hartree–Fock approximation). In [8] it was shown how a correlation correction, often referred to as the Lam–Platzman [9] term can be determined within the local density approximation (LDA) and recently [10] the method has been extended to cope with a wider range of electron densities.

Whilst the Lam–Platzman term considerably improves the agreement between individual experimental and theoretical profiles, it is necessarily isotropic and therefore has no effect at all on the directional differences $\Delta J(p)$. Inspection of the individual profiles reveals that the discrepancy arises from a preferential expansion of the momentum density along the nearest-neighbour direction, a feature which cannot be modelled within the framework of the LDA. In this paper a novel method of calculating anisotropic correlation corrections from the three-dimensional density $N(\boldsymbol{k})$ of states is employed.

Previously, Compton scattering studies of chromium had been made on single crystals [11] and on a polycrystal [12] with 60 keV ^{241}Am γ-radiation. Data sets with a point-by-point statistical accuracy of about 1% were obtained in both cases. Although the single-crystal data were adequate to establish the directional differences, which amount to 5% of $J(0)$ at low momenta, the extraction of the individual profiles is more uncertain because of the problematical nature of several systematic corrections, and also the obvious failure of the impulse approximation for the K-shell electrons (the mean energy transfer is only twice the K-shell binding energy). The precision of the data was inadequate for probing subtle correlation effects.

The isotropic (polycrystalline sample) profile was compared with the results of a renormalised free-atom model based on the $3d^4 4s^2$ configuration and the single-crystal data with a linear combination of atomic orbitals (LCAO) [13] calculation which predicted larger anisotropies than were observed throughout the entire momentum range. Since then an augmented plane-wave (APW) calculation has appeared [14] which is based on a modified X_α potential; it predicts anisotropies midway between the LCAO model and the data.

Systematic data corrections are now better understood and can be applied more precisely, especially if the experiments are carried out with a high-energy source such as ^{198}Au ($E_\gamma = 412$ keV) which produces 50% better momentum resolution and a more straightforward interpretation [1]. It was therefore decided to make a single-crystal study of chromium at room temperature (i.e. below the magnetic transition at 311 K) to complement the published ^{198}Au studies of vanadium, iron, nickel and copper.

2. Data analysis

The majority of the data reported below were collected on the ^{198}Au Compton spectrometer sited at the Rutherford Appleton Laboratory and described elsewhere [15]. Details of the ^{241}Am spectrometer at the University of Warwick used for the lower-energy

Table 1. Compton spectrometers: experimental details for chromium.

Parameter	Rutherford Appleton Laboratory	University of Warwick
Isotope and γ-ray energy	^{198}Au, 411.8 keV	^{241}Am, 59.5 keV
Half-life	2.7 d	452 a
Initial activity	150 C	5 C
Time for typical 3×10^7 counts, integrated Compton intensity	60–180 h	360 h
Scattering angle	$167 \pm 1°$	$170.5 \pm 1°$
Electron momentum resolution ($1 \text{ au} = 1.99 \times 10^{-24} \text{ kg m s}^{-1}$)	0.40 au	0.57 au
Disc sample sizes	9–11 mm diameter 2–2.2 mm thick	9–11 mm diameter 2–2.2 mm thick
Compton peak: background ratio	400:1	100:1
Percentage of multiple scattering	15–18%	13%

measurements can be found in [16]; the important parameters of both spectrometers are summarised in table 1.

The Compton line (equation (1)) is inherently symmetric; therefore the final symmetry of the processed profile is usually regarded as an acid test of the data processing. In fact, there are so many energy-dependent corrections involved in the data analysis, some of which may be compensatory, that centrosymmetry is a necessary but not sufficient guarantee of validity. In practice the most elusive corrections are concerned with the following:

(i) the detector response function which always has a low-energy tail;
(ii) Compton scattering within the source which has a similar effect;
(iii) the energy dependence of the detector efficiency (for ^{198}Au experiments only);
(iv) parasitic multiple scattering which is a long-standing and well chronicled problem.

In [17], (i) and (ii) were considered especially for the lower-energy experiment where the problem is compounded by the fact that the resolution function cannot easily be measured at the Compton peak energy (48.6 keV). In contrast the ^{198}Au spectrometer is designed so that the peak occurs at 159 keV which is the γ-ray emission energy of the ^{123m}Te isotope; even then the measurement of an appropriate response function depends on mimicking the sample–detector geometry. The correction is better assured, however, than in the ^{241}Am case where the 60 keV resolution function is usually taken to represent the 48 keV response convoluted with beam divergence effects. In addition, its considerable variation across the profile is usually neglected; this problem is much less acute in the higher-energy experiment as is the self-scattering contamination of the incident beam which was also investigated in [7].

All these arguments, together with the obvious breakdown of the impulse approximation for the chromium K-shell electrons ($E_B = 5.9$ keV) in the ^{241}Am experiment lead to the conclusion that symmetric directional profiles will not be forthcoming in this experiment. The data should only be used for confirming the directional differences, as concluded in earlier dual-energy studies on aluminium [18].

The correction of the ^{198}Au data for multiple scattering then proceeds by the well known, if time-consuming, Monte Carlo method originally adopted for this problem [19]. It is assumed that the multiple-scattering spectrum would not be directionally

dependent but that sample thickness differences (2.0 and 2.2 mm were used) would matter. In each simulation, 4×10^6 photons were inputted in order to obtain more than 10^4 multiply scattered photons in the energy range of interest.

The net results of all these procedures, together with the more routine processing corrections not elaborated on here, is a set of ^{198}Au chromium profiles with asymmetry, expressed as $[J(+p_z) - J(-p_z)]/J(0)$ which is less than 2.5×10^{-3} over the majority of the range $-10 < p < +10$ au. This meant that data from both the low-energy and the high-energy side of the profile could be used for the first time to form the absolute profiles. The point-by-point random error for data interpolated at 0.1 au intervals was estimated as $4 \times 10^{-3} J(0)$ at low momenta where the limitations in statistical accuracy are most important.

3. Experiment and theory compared

The LCAO calculation [13] uses five Gaussian-type orbitals to describe the 3d electrons and determines the Bloch functions $u_k(\boldsymbol{r})\exp(i\boldsymbol{k}\cdot\boldsymbol{r})$ at 140 points in the irreducible element of the Brillouin zone. The momentum density $n(\boldsymbol{p})$ is then calculated from an expansion over 3000 reciprocal lattice vectors $\boldsymbol{G}$, i.e.

$$n(\boldsymbol{p}) = \sum_{G}\sum_{k} n(\boldsymbol{k})|V_G(\boldsymbol{k})|^2\delta(\boldsymbol{G}+\boldsymbol{k}-\boldsymbol{p}) \tag{2}$$

where $V_G(\boldsymbol{k})$ is the Fourier coefficient of $u(\boldsymbol{r})$ and $n(\boldsymbol{k})$ represents the band occupation number of the state $\boldsymbol{k}$ (i.e. 1 or 0 in the independent particle approximation).

The original APW calculation [14], which used spherical harmonics up to $l = 6$, was limited to a reciprocal lattice expansion over 87 terms so that $n(\boldsymbol{p})$ was calculated out to a limit of $|\boldsymbol{p}| < 4$ au which did not encompass the entire 3d electron distribution (about 0.16 electrons remained unaccounted for). Unfortunately, this means that the Compton profile (equation (1)) is slightly deficient at all momenta. The APW profiles have now been recalculated [20] using the same modified potential but with the expansion extended to 756 terms; this now reproduces the correct profile normalisation. The recalculated profile is very close to the LCAO values as can be judged from table 2. (Note that both theoretical profiles quoted in table 2 have been convoluted with a Gaussian full width at half-maximum (FWHM) of 0.40 au to bring them to the same resolution as the experiment.)

3.1. The directional difference profiles and Fermi surface geometry

In common with other transition metals the oscillations of the difference profiles are qualitatively governed by the geometry of the Fermi surface, the scale rather than the pitch depending on the detailed wavefunctions. The Fermi surface in the third, fourth and fifth zones is shown in figure 1. In contrast with vanadium there is no multiply connected jungle-gym hole surface in the third zone of chromium; it is reduced to separate octahedral holes at the H points (plus small hole pockets at N). In the fourth zone the major feature is the electron jack at the Γ point. Remembering that the Compton profile is a set of integrals over planes perpendicular to the scattering vector, we can see that both $J_{100}(0)$ and $J_{110}(0)$ are integrals over planes which intersect the holes in the third zone and the electron jack in the fourth zone; these effects roughly cancel and both profiles are therefore similar. This is not true for $J_{111}(0)$ which misses the hole

Table 2. The experimental and theoretical Compton profiles of chromium. The model profiles have been convoluted with a Gaussian of FWHM = 0.40 au to match them to the experimental data. The free-atom profile is taken from [21].

	[100]			[110]			[111]			
		Band theories			Band theories			Band theories		Free-atom
p_z (au)	Experiment	APW	LCAO	Experiment	APW	LCAO	Experiment	APW	LCAO	value
0.0	5.017 ± 0.019	5.099	5.107	5.162	5.269	5.258	5.266	5.459	5.462	5.789
0.1	5.008	5.086	5.092	5.147	5.248	5.237	5.240	5.414	5.418	5.685
0.2	4.971	5.045	5.046	5.077	5.185	5.173	5.157	5.289	5.295	5.413
0.3	4.900	4.979	4.972	4.967	5.079	5.068	5.020	5.109	5.111	5.064
0.4	4.795	4.877	4.870	4.821	4.939	4.925	4.852	4.904	4.896	4.725
0.5	4.666	4.747	4.741	4.653	4.754	4.753	4.656	4.696	4.677	4.445
0.6	4.497	4.585	4.587	4.466	4.551	4.561	4.436	4.492	4.469	4.224
0.7	4.308	4.395	4.410	4.254	4.332	4.358	4.223	4.289	4.275	4.043
0.8	4.108	4.180	4.212	4.093	4.106	4.148	4.016	4.082	4.087	3.878
0.9	3.887	3.942	3.995	3.806	3.876	3.931	3.811	3.862	3.892	3.713
1.0	3.648	3.688	3.762	3.584	3.644	3.706	3.587	3.626	3.676	3.642
1.2	3.166	3.177	3.267	3.127	3.166	3.233	3.120	3.122	3.186	3.177
1.4	2.739	2.733	2.797	2.701	2.702	2.766	2.700	2.670	2.734	2.805
1.6	2.357	2.349	2.380	2.318	2.305	2.359	2.349	2.318	2.383	2.449
1.8	2.020	2.007	2.017	2.013	1.983	2.022	2.027	2.011	2.059	2.126
2.0	1.769	1.733	1.742	1.762	1.720	1.748	1.765	1.736	1.764	1.844
2.5	1.307	1.277	1.308	1.290	1.267	1.283	1.280	1.249	1.260	1.315
3.0	0.990	0.954	0.969	0.992	0.954	0.969	0.994	0.963	0.985	0.990
3.5	0.795	0.763	0.790	0.798	0.762	0.785	0.795	0.758	0.782	0.788
4.0	0.687	0.642	0.649	0.682	0.642	0.647	0.678	0.643	0.653	0.656
5.0	0.520 ± 0.005	0.489	0.480	0.528	0.488	0.481	0.515	0.487	0.481	0.485
6.0	0.396		0.364	0.406		0.364	0.392		0.364	0.369
7.0	0.299			0.300			0.283			0.282
10.0	0.155 ± 0.032			0.157			0.153			0.130

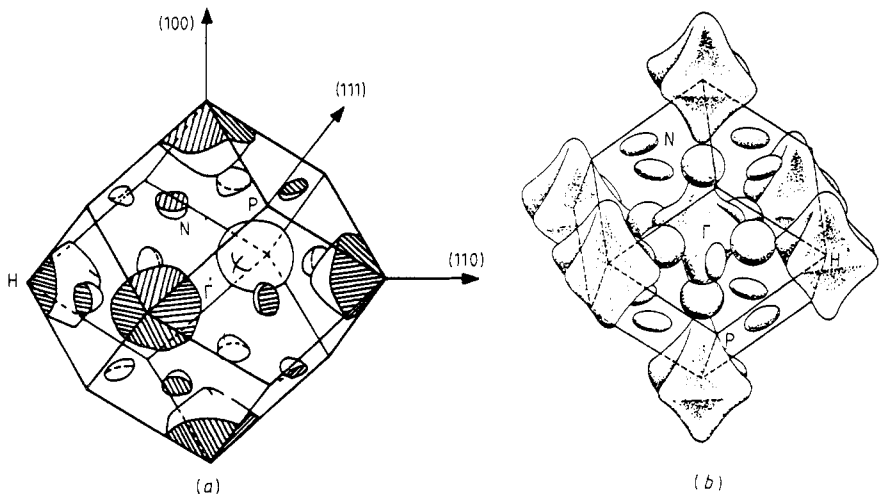

Figure 1. The Fermi surface of chromium: (*a*) closed hole pockets at N and H in the third band (from [14]); (*b*) the electron contribution to the fourth and fifth bands (from [22]).

surfaces but intersects those at H when $p = 2\pi/a\sqrt{3} = 0.69$ au and thus varies from being the largest to the smallest profile over that range.

The observed directional difference profiles derived from the ^{198}Au experimental data are shown in figure 2. The predictions of APW and LCAO calculations are inseparable

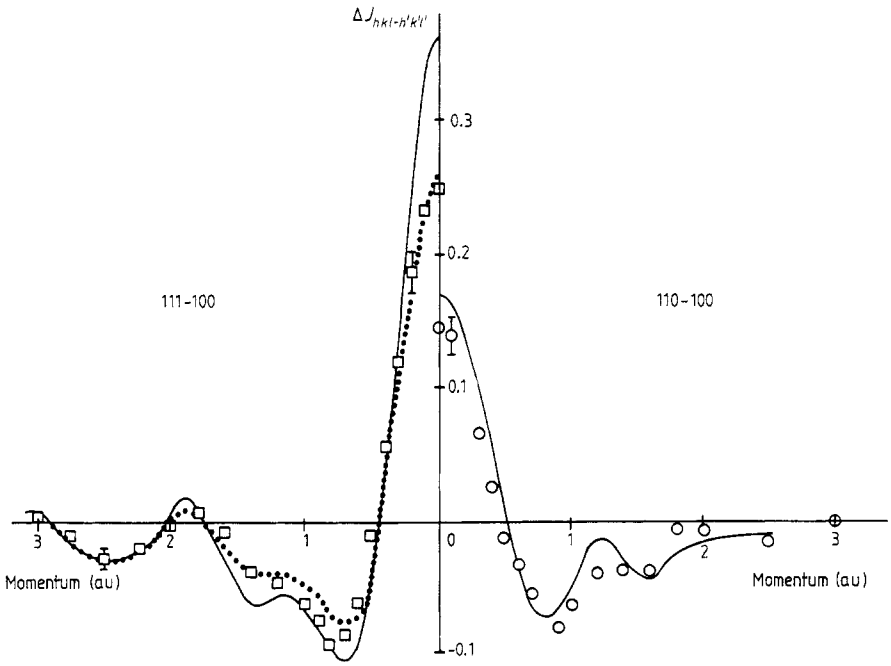

Figure 2. The directional difference Compton profiles of chromium deduced from the ^{198}Au source data: ———, the difference predicted by the APW model at the experimental resolution (see table 2); · · · ·, the effect of incorporating the correlation correction listed in table 3.

on this scale; therefore only one curve, which is based on the APW numbers, is shown. Qualitatively all the features evident in the higher-resolution data set correspond closely to the predicted curve. The ^{241}Am results, not reproduced here, confirm the ^{198}Au data but show smaller oscillations because of the more severe resolution broadening (see table 1); features such as the small local maxima at around $p = 1$ au are consequently washed out. The APW calculation reveals a preferential (72%) occupation of t_{2g} orbitals which point along the nearest-neighbour [111] directions. Planes through the origin perpendicular to [110] and [111] therefore intersect greater momentum density than [100].

The detailed agreement between experiment and theory for the [110]–[100] directional difference strongly indicates that the discrepancies are associated with the [111] direction. In fact, it transpires that they are entirely due to the anisotropic correlation effects which will be discussed in § 3.2.

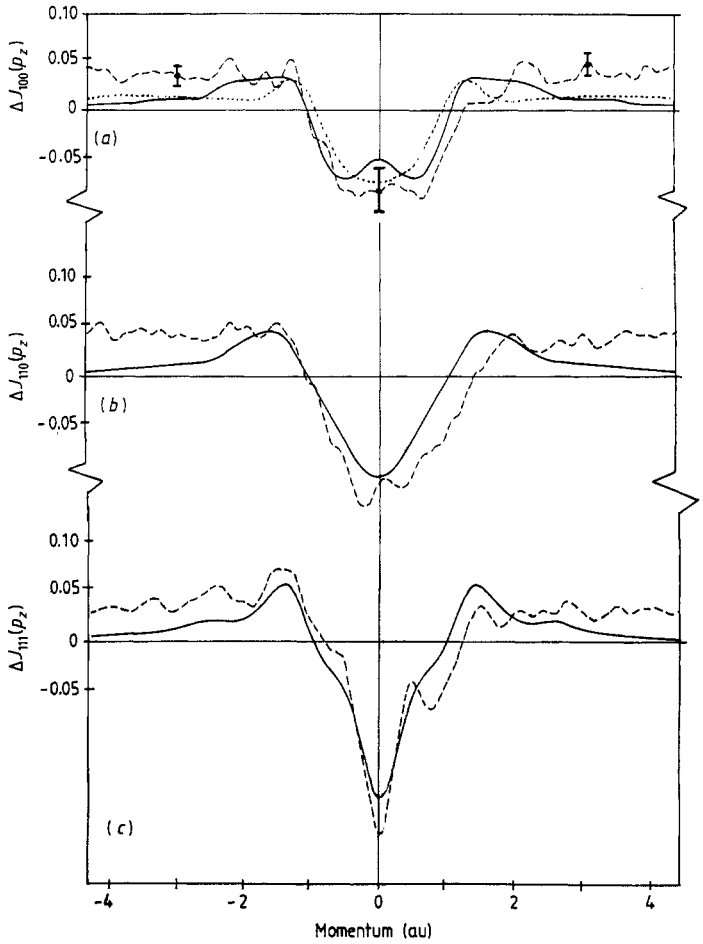

Figure 3. The individual Compton profiles (– – –) for each of the principle cubic directions ((*a*) [100]; (*b*) [110]; (*c*) [111]) after subtraction of the APW model profile. Typical experimental errors are indicated in (*a*). In each case the model is too large at low momenta ($p_z < 1$ au). The correlation correction [23] calculated from equation (4) is also given. The isotropic Lam–Platzman correction [10] (· · · ·) is shown in (*a*) only.

3.2. Electron correlation effects and individual directional profiles

In general terms, electron–electron correlation effects will promote electrons to higher-momentum states so that for an interacting electron gas the occupation numbers will not be either 1 or 0 depending on whether the state is below or above the Fermi surface, but some continuous function $n(p)$. In terms of the Compton profile this means a transfer of density from low ($p < p_F$) to high ($p > p_F$) momentum. A cursory inspection of table 2 shows that this is what is needed to bring theory close in line with experiment. This is very obvious from figure 3 where the differences between the directional profiles and the APW predictions are plotted (broken curves).

Within the LDA the isotropic Lam–Platzman correction can be calculated using the occupation numbers for an interacting electron gas [23–25]. This has been done by one of us [10] and produces a first-order improvement between experiment and theory as can be seen in figure 3 where the Lam–Platzman term has been superimposed on the 100 residual difference. It matches it fairly accurately and is similarly close to the residual difference for 110. However, it is much too small to reconcile experiment and theory for the [111] direction as anticipated by the discrepancy in the [111]–[100] directional difference curve in figure 2 which is, of course, insensitive to isotropic terms.

In a new approach developed by one of us [26] the occupation numbers of the correlated electron gas, the so-called Migdal [23] function is transformed to a function of energy $n(E)$.

The profile is then calculated by summing over all electron energy states which contribute to each profile at a particular momentum, i.e.

$$J(p) = \sum_{\Gamma_1}^{\infty} n(E)J(p, E)\,\Delta E \tag{3}$$

where $n(E)$ is now non-zero for $E > E_F$ and the states are summed from the origin Γ_1 at the centre of the Brillouin zone. The equivalent of the Lam–Platzman correction term is therefore

$$\Delta J_{corr}(p) = \sum_{E=\Gamma_1}^{E_F} [1 - n(E)]J(p, E)\,\Delta E + \sum_{E_F}^{\infty} n(E)J(p, E)\,\Delta E \tag{4}$$

which is now directionally dependent since the states are distributed anisotropically throughout the Brillouin zone. The calculation is not from first principles because of the modelling of $n(E)$ but it provides an accurate correction in chromium and also vanadium (for further details see [26]). This is demonstrated in figure 2 for the directional differences by the close fit between the data points and the dotted curve which includes this correction to the APW curve. It is also evident in figure 3 where it can be seen that this correlation correction to the [111] prediction is quite different from those for the two other orientations. In all three cases the correction (broken curves) accurately describes the residual discrepancies between experiment and theory at low momenta to the extent of reproducing detailed features such as the local maximum at $p = 0$ in the [100] data and the shoulder at $p \simeq 0.5$ au in the [111] data. The directional Compton profiles together with this correlation correction derived from the APW calculation are listed in table 3; this time the data are not smeared by the experimental resolution function.

It should be mentioned that figure 3 illustrates a defect in the absolute profile data which is that the experimental profile high-momentum tails are too large, i.e. they exceed the free-atom values by one or two standard deviations. This problem was also evident

Table 3. The correlation correction to the directional Compton profiles of chromium calculated by Wakoh and Matsumoto [26]. The first set of values for each orientation is without experimental broadening and the second set is convoluted with a Gaussian of FWHM = 0.40 au.

	100		110		111	
p_z (au)	Without experimental broadening	Convoluted with a Gaussian	Without experimental broadening	Convoluted with a Gaussian	Without experimental broadening	Convoluted with a Gaussian
0	−0.044	−0.0500	−0.097	−0.097	−0.176	−0.148
0.1	−0.049	−0.051	−0.099	−0.095	−0.165	−0.140
0.2	−0.054	−0.054	−0.099	−0.092	−0.128	−0.119
0.3	−0.055	−0.058	−0.090	−0.084	−0.088	−0.092
0.4	−0.067	−0.061	−0.077	−0.074	−0.045	−0.065
0.5	−0.067	−0.062	−0.060	−0.061	−0.034	−0.045
0.6	−0.060	−0.060	−0.046	−0.048	−0.022	−0.032
0.7	−0.063	−0.056	−0.033	−0.036	−0.019	−0.025
0.8	−0.055	−0.048	−0.022	−0.026	−0.026	−0.020
0.9	−0.043	−0.036	−0.016	−0.016	−0.023	−0.013
1.0	−0.027	−0.020	−0.011	−0.007	−0.016	−0.003
1.2	+0.023	+0.013	+0.012	+0.015	+0.032	+0.028
1.4	0.033	0.029	0.043	0.035	0.063	0.048
1.6	0.028	0.033	0.046	0.042	0.042	0.045
1.8	0.038	0.034	0.039	0.040	0.034	0.035
2.0	0.029	0.030	0.035	0.034	0.027	0.027
2.5	0.013	0.015	0.013	0.015	0.017	0.017
3.0	0.013	0.012	0.013	0.012	0.008	0.011
3.5	0.008	0.008	0.007	0.008	0.008	0.008
4.0	0.005	0.005	0.005	0.005	0.005	0.005
5.0	0.002	0.002	0.002	0.002	0.002	0.002

in the earlier Rutherford Appleton Laboratory data on nickel [7] and may arise from a recently detected low radiation background from adjacent laboratories. Without this parasitic contribution the agreement might be even better. Fortunately, it does not affect the improved agreement of experimental and theoretical directional difference curves.

It may be concluded that Compton scattering experiments are capable of identifying anisotropic correlation effects in transition metals which are pronounced when the Fermi surface lies in the middle of the d bands. Conventional band theory, together with the description of correlation affects outlined here, can provide an accurate description of the momentum density distribution.

Acknowledgments

The authors are indebted to the Science and Engineering Research Council for their overall support of this project and for a visiting fellowship (SW) and a research studentship (DAC). We are grateful to Mr I Bailey and other staff at the Rutherford Appleton Laboratory for their assistance and to Dr R S Holt, Dr D Laundy and Mr D N Timms for many useful discussions.

References

[1] Cooper M J 1985 *Rep. Prog. Phys.* **48** 45
[2] Mijnarends P E 1977 *Compton Scattering* ed. B E Williams (New York: McGraw-Hill) ch 10
[3] Rollason A J, Holt R S and Cooper M J 1983 *Phil. Mag.* B **47** 51
[4] Rollason A J, Holt R S and Cooper M J 1983 *J. Phys. F: Met. Phys.* **13** 1807
[5] Bauer G E W and Schneider J R 1983 *Z. Phys.* B **54** 17
[6] Bauer G E W and Schneider J R 1984 *Phys. Rev. Lett.* **52** 2061
[7] Rollason A J, Schneider J R, Laundy D, Holt R S and Cooper M J, 1987 *J. Phys. F: Met. Phys.* **17** 1105
[8] Bauer G E W 1984 *Phys. Rev.* B **30** 1010
[9] Lam L and Platzman P 1974 *Phys. Rev.* B **9** 5122
[10] Cardwell D A 1987 *PhD Thesis* University of Warwick
[11] Ohara S, Fukamachi T, Hosoya S and Takeda T 1974 *J. Phys. Soc. Japan* **35** 337
[12] Paarkari T, Manninen S O and Berggren K-F 1975 *Phys. Fenn.* **10** 207
[13] Rath J, Wang C S, Tawil R A and Callaway J 1973 *Phys. Rev.* B **8** 5139
[14] Wakoh S, Kubo Y and Yamashita J 1976 *J. Phys. Soc. Japan* **40** 1043
[15] Holt R S, Cooper M J, DuBard J L, Forsyth J B, Jones T L and Knights K 1979 *J. Phys. E: Sci. Instrum.* **12** 1148
[16] Cooper M J, Holt R S and DuBard J L 1978 *J. Phys. E: Sci. Instrum.* **11** 1145
[17] Manninen S O, Cooper M J and Cardwell D A 1986 *Nucl. Instrum. Methods* A **245** 485
[18] Cardwell D A and Cooper M J 1986 *Phil. Mag.* B **54** 37
[19] Felsteiner J, Pattison P and Cooper M J 1974 *Phil. Mag.* **30** 537
[20] Wakoh S 1986 private communication
[21] Biggs F, Mendelson L B and Mann J B 1975 *At. Data Nucl. Data Tables* **16** 201
[22] Cracknell A P and Wong K C 1973 *The Fermi Surface* (Oxford: OUP)
[23] Migdal A B 1957 *Sov. Phys.–JETP* **5** 333
[24] Lundqvist B I 1967 *Phys. Kondens. Mater.* **7** 117
[25] Rennert P 1981 *Phys. Status Solidi* **105** 567
[26] Wakoh S and Matsumoto M 1988 private communication